

UNIVERSIDAD SAN FRANCISCO DE QUITO USFQ

Colegio de Ciencias e Ingenierías

**Parametric study on the applicability of AASHTO LRFD for
simply supported reinforced concrete slab bridges**

Lucía Moya Tamariz

Ingeniería Civil

Trabajo de fin de carrera presentado como requisito
para la obtención del título de
Ingeniero Civil

Quito, 3 de mayo de 2021

UNIVERSIDAD SAN FRANCISCO DE QUITO USFQ

Colegio de Ciencias e Ingenierías

**HOJA DE CALIFICACIÓN
DE TRABAJO DE FIN DE CARRERA**

**Parametric study on the applicability of AASHTO LRFD for
simply supported reinforced concrete slab bridges**

Lucía Moya Tamariz

Nombre del profesor, Título académico

Eva O.L. Lantsoght, PhD.

Quito, 3 de mayo de 2021

© DERECHOS DE AUTOR

Por medio del presente documento certifico que he leído todas las Políticas y Manuales de la Universidad San Francisco de Quito USFQ, incluyendo la Política de Propiedad Intelectual USFQ, y estoy de acuerdo con su contenido, por lo que los derechos de propiedad intelectual del presente trabajo quedan sujetos a lo dispuesto en esas Políticas.

Asimismo, autorizo a la USFQ para que realice la digitalización y publicación de este trabajo en el repositorio virtual, de conformidad a lo dispuesto en la Ley Orgánica de Educación Superior del Ecuador.

Nombres y apellidos: Lucía Moya Tamariz

Código: 00136292

Cédula de identidad: 1722735915

Lugar y fecha: Quito, 3 de mayo de 2021

ACLARACIÓN PARA PUBLICACIÓN

Nota: El presente trabajo, en su totalidad o cualquiera de sus partes, no debe ser considerado como una publicación, incluso a pesar de estar disponible sin restricciones a través de un repositorio institucional. Esta declaración se alinea con las prácticas y recomendaciones presentadas por el Committee on Publication Ethics COPE descritas por Barbour et al. (2017) Discussion document on best practice for issues around theses publishing, disponible en <http://bit.ly/COPETHeses>.

UNPUBLISHED DOCUMENT

Note: The following capstone project is available through Universidad San Francisco de Quito USFQ institutional repository. Nonetheless, this project – in whole or in part – should not be considered a publication. This statement follows the recommendations presented by the Committee on Publication Ethics COPE described by Barbour et al. (2017) Discussion document on best practice for issues around theses publishing available on <http://bit.ly/COPETHeses>.

Para mi abuelo y ángel Guillermo Tamariz

AGRADECIMIENTOS

Quiero empezar agradeciendo a mi ñaño, que aunque es de pocas palabras, siempre está ahí para lo que necesite; a mi ma, que no sé de dónde saca tanta energía para trabajar unas diez horas diarias y aún así hacer todo por nosotros; y a mi pa, que aunque no comparto su afición por las vías, me inspiró a desarrollar la estima que tengo por mi carrera.

De la misma manera, quisiera agradecer a Eva Lantsoght, directora de este trabajo de titulación, por haber sido una guía tan sólida en todo este proceso.

Gracias también a mis amigos y en especial a Angie Moya. La universidad no hubiera sido lo mismo sin ustedes, y este último año y medio de no compartir las mismas clases me lo confirmó.

Finalmente, gracias Nicolás por haber aparecido en mi vida un 29 de noviembre de hace más de cuatro años. Sentarme en la última fila del cine en Química para jugar Octagon fue la mejor decisión que tomé en la universidad.

RESUMEN

En este artículo se presentan los resultados de un estudio paramétrico para determinar la aplicabilidad de AASHTO LRFD para puentes losa esviados simplemente apoyados de hormigón armado, con el refuerzo longitudinal principal paralelo a la dirección del tráfico. Un total de 80 casos de estudio, cuyos parámetros que varían son longitud, ancho y ángulo de esviaje, se someten a la carga AASHTO HL-93. Los puentes se analizan usando los procedimientos simplificados AASHTO LRFD, por medio de cálculos manuales, y usando LFEA del paquete de software SCIA Engineering. La provisión de refuerzo en términos de refuerzo longitudinal principal, transversal secundario y a cortante se determina de acuerdo con las especificaciones para diseño de AASHTO LRFD para los dos métodos de análisis mencionados. En comparación con el análisis AASHTO LRFD, a medida que el ángulo de esviaje aumenta, LFEA produce momentos de flexión más bajos y más altos en las direcciones paralela y perpendicular al tráfico, respectivamente, así como fuerzas de corte más altas en la esquina obtusa. Esto da como resultado una disminución del refuerzo longitudinal principal, un aumento del refuerzo transversal secundario y un impacto negativo en la relación entre la demanda de cortante y la capacidad de cortante, que puede llevar a la necesidad de refuerzo de cortante mínimo en la esquina obtusa. Además, para la mayoría de los puentes, los anchos de distribución para cargas vivas proporcionados por LFEA sugieren que se pueden proporcionar los mismos espaciamientos o diámetros de varilla para el refuerzo longitudinal principal a lo largo de todo el ancho del puente. En consecuencia, cuando se aplica al diseño de puentes losa esviados, LFEA es más aconsejable que los procedimientos simplificados AASHTO LRFD por cuestiones de reducción de costos, cuando se habla de refuerzo longitudinal principal, y cuestiones de seguridad, cuando se habla de refuerzo secundario transversal y a cortante.

Palabras clave: puentes losa; hormigón armado; ángulo de esviaje; refuerzo longitudinal principal; refuerzo secundario transversal; refuerzo a cortante; distribución de carga viva.

ABSTRACT

Results of a parametric study on the applicability of AASHTO LRFD for simply supported reinforced concrete skewed slab bridges, with main longitudinal reinforcement parallel to the direction of the traffic, are presented in this paper. A total of 80 case study bridges, whose varying parameters are length, width, and skew angle, are subjected to the AASHTO HL-93 loading. The bridges are analyzed using the AASHTO LRFD simplified procedures, using hand calculations, and LFEA from the software package SCIA Engineering. Reinforcement provision in terms of main longitudinal, secondary transverse, and shear reinforcement is determined according to the AASHTO LRFD for the analysis methods mentioned herein. In comparison to AASHTO LRFD analysis, as the skew angle increases LFEA yields lower and higher bending moments in the parallel and perpendicular directions of the traffic, respectively, as well as higher shear forces at the obtuse corner. This results in decreased main longitudinal reinforcement, increased secondary transverse reinforcement, and a negative impact on the relation between shear demand and shear capacity, which can lead to the need for minimum shear reinforcement at the obtuse corner. Additionally, for the majority of bridges, the widths of distribution for live loading yielded by LFEA suggest that the same spacings or bar diameters for the main longitudinal reinforcement can be provided along the entire width of the bridge. In consequence, when applied to the design of skewed slab bridges, LFEA is preferable over AASHTO LRFD simplified procedures for cost reduction concerns, regarding main longitudinal reinforcement, and safety concerns, regarding secondary transverse and shear reinforcement.

Keywords: slab bridges; reinforced concrete; skew angle; main longitudinal reinforcement; secondary transverse reinforcement; shear reinforcement; live load distribution.

CONTENTS

INTRODUCTION.....	12
DEVELOPMENT OF THE TOPIC	16
1. Materials and Methods.....	16
1.1. Design of the Parameter Studies.....	16
1.2. Analysis and Design Procedures.....	17
1.2.1. AASHTO LRFD hand calculation.....	17
1.2.2. Use of linear finite element models	20
2. Results and Analysis.....	24
2.1. Influence of Steel Yield Strength and Concrete Compressive Strength	25
2.2. Maximum main longitudinal bending moment	26
2.3. LFEA live load distribution width for main longitudinal bending moment.....	29
2.4. Maximum secondary transverse bending moment	30
2.5. Shear demand versus shear capacity.....	33
2.6. Particular case study bridges	34
2.7. Weight of steel reinforcement comparison.....	36
3. Discussion.....	38
CONCLUSIONS	42
REFERENCES.....	45
APPENDIX A: NOTATION.....	47

LIST OF TABLES

Table 1. Matrix of parameters studied	17
Table 2. Multiple presence factors (AASHTO, 2017)	21
Table 3. Interior and exterior strip $M_{l,max}$ overestimation and $M_{l,max}$ reduction percentage per AASHTO LRFD and LFEA.....	28
Table 4. Increase in LFEA $M_{t,max}$ demand versus AASHTO LRFD capacity	31
Table 5. Reinforcement provision for the 7.5 m long, 4 lanes, 15° skew case study bridge with different material properties	35
Table 6. Reinforcement provision for the 15 m long, 2 lanes, 45° skew case study bridge with different material properties	35

LIST OF FIGURES

Figure 1. Geometric definition of length, width, and skew angle.....	16
Figure 2. Cross section scheme for the one lane case study bridge.....	16
Figure 3. Principle of the effective width applied both to moment and shear determination (Lantsoght, 2013).	21
Figure 4. Main longitudinal and secondary transverse moment section cuts for design. (a) Straight bridges; (b) Skewed bridges.	22
Figure 5. Shear section cuts for design. (a) Straight bridges; (b) Skewed bridges.	23
Figure 6. Comparison of LFEA and AASHTO LRFD maximum main longitudinal bending moment. (a) L = 7.5 m; (b) L = 10 m; (c) L = 12.5 m; (d) L = 15 m.	27
Figure 7. Trajectories of the principal stresses for the 12 m long, 2 lanes case study bridge. (a) Straight $\alpha = 0^\circ$; (b) Skewed $\alpha = 60^\circ$	28
Figure 8. <i>Relation of effective width of distribution for live load, yielded by LFEA, to width of bridge.</i>	29
Figure 9. Comparison of LFEA maximum secondary transverse bending moment and AASHTO LRFD bending moment capacity achieved by distribution reinforcement provision. (a) L = 7.5 m; (b) L = 10 m; (c) L = 12.5 m; (d) L = 15 m.	32
Figure 10. Relation of shear demand to concrete shear capacity with no shear reinforcement.	33
Figure 11. Weight steel reinforcement for bending moment comparison. (a) Main longitudinal; (b) Secondary transverse.	36
Figure 12. Difference between LFEA and AASHTO LRFD of the summation, in weight, of $M_{I,max}$ and $M_{t,max}$ steel reinforcement.	38

INTRODUCTION

AASHTO defines a bridge as a structure with an opening greater than 6.10 m (20.0 ft), that is either a component of a highway or is located above or under a highway (AASHTO, 2017). Bridges can be classified by their superstructure as slab, beam or girder, arch, truss, cable stayed, and suspension, and the name refers to the main spanning structural component. One of the most decisive factors when selecting a bridge type is the distance to be spanned. Slab bridges, for instance, are chosen when the avoidance of beams results cost-effective compared to beam or girder bridges: this generally occurs for short spans (Fu, 2013). Despite the limitation in span length, slab bridges are widely used worldwide. In fact, according to the U.S. Federal Highway Administration's 2020 National Bridge Inventory data, nearly 65000, out of the nationwide registered 619000 highway bridges, are classified as concrete slab bridges with a maximum span length averaging less than 10 m (US. FedHighAdm, 2020). Moreover, slab bridges offer a large shear capacity (Fu, 2013).

Slab bridges can be straight or skewed, which means that the main longitudinal direction of the bridge can be perpendicular to the support line, i.e., straight slab bridge with 0° skew angle, or a deviation of the main longitudinal direction from the vertical axis can occur, i.e., skewed slab bridge with skew angle greater than 0° , (see Figure 1). Even though skewed slab bridges are not ideal structurally speaking, due to the significant increase of shear forces concentrated at the obtuse corners, they are common when spatial constraints, either urban or geographical, prevent the design of straight geometries.

AASHTO LRFD Bridge Design Specifications (AASHTO LRFD) allow simply supported solid slab bridges, with main longitudinal reinforcement parallel to the direction of the traffic, to be designed using simplified methods that divide the superstructure into a series

of interior and exterior beam type elements (AASHTO, 2017). As well, the specifications propose a reduction factor to be applied for bending moments as the skew of the bridge increases; however, no additional considerations regarding skewness are taken when analyzing shear (AASHTO, 2017). Even so, limited attention had been paid to skewed solid slab bridges, since they were generally considered as one-way slabs where the longitudinal moments are carried by the main longitudinal reinforcement and the transverse moments are carried by the secondary transverse reinforcement calculated with empirical expressions (Théoret et al., 2012).

However, the collapse of the Concorde Overpass (Massicotte, 2007), that caused five fatal casualties and the injury of six people, drew attention to the safety, regarding shear strength, of solid concrete slabs and, particularly, of those that were skewed (Hulsebosch, 2019). This unfortunate event led to several conclusions regarding bridge design, and the following two of them are the most relevant to this study. First, simplified analysis methods should be more restrictive to ensure that bridges with high skew angles are analyzed with more detailed methods. Second, standards should ask for minimum shear reinforcement in thick slabs that work as the main spanning structural component (Mitchell, 2011).

Several parametric studies regarding skewed slab bridges have been performed with the objective comparing simplified to more refined analysis methods. Théoret conducted a parametric study on 390 simply supported slabs and established a series of expressions to develop moment reduction factors and shear magnification factors to compensate for skewness when using the simplified analysis procedures from AASHTO LRFD (Théoret et al., 2012). Menassa analyzed 96 case study bridges using the AASHTO Standard Specifications, AASHTO LRFD and FEA. It was determined that AASHTO Standard Specifications yield similar results of maximum longitudinal bending moment to FEA for skew angles smaller than

20°; however, the overestimation increased up to 100% as the skew angle reached to 50°. As well, the overestimation produced by AASHTO LRFD for a skew angle less than 30° went up to 40%, and even 50% as the skew angle reached 50° (Menassa, 2007). Sharma, on the other hand, developed a predictive modeling method for reinforced concrete skewed slabs. The model accurately predicted ultimate flexural capacity, as well as flexural response, for most of the tested skews (Sharma, 2019). Nonetheless, even if shear behavior has been investigated for a long time, there is no clear agreement on how to define a single shear design approach. In consequence, Lipari proposed and validated a procedure to extend code shear design provisions to skewed geometries (Lipari, 2019), and this procedure is selected for shear design purposes of this study.

The aim this paper is twofold. First, this study aspires to give an insight on how skewness affects the magnitudes of main longitudinal and secondary transverse bending moments at midspan, and shear forces at the critical shear section close to the obtuse corner. Also, parallel to comparing these magnitudes, a distinction is intended to be made as to when the differences in magnitudes signify higher or smaller amounts of reinforcement, and when the amount of reinforcement is not affected. As such, this work gives practical and relevant insights on the effects of skew for the designer. Second, the study pretends to contrast the width of distribution for the live load using LFEA with the width of the bridge to determine when the same spacings or bar diameters for the main longitudinal reinforcement can be provided along the entire width of the bridge. In addition, this work provides insights in the difference between hand calculations per AASHTO LRFD and the more refined LFEA.

The outcome of the parametric study leads to conclude that as the skew angle increases, the main longitudinal reinforcement decreases, the secondary transverse reinforcement increases, and minimum shear reinforcement at the obtuse corner could become necessary.

Additionally, for the majority of bridges, it appears that the same spacings or bar diameters for the main longitudinal reinforcement can be provided along the entire width of the bridge due to the widths of distribution for live loading obtained with LFEA.

DEVELOPMENT OF THE TOPIC

1. Materials and Methods

1.1. Design of the Parameter Studies

There are three geometric parameters to be studied: length (L), width (W), and skew angle (α), and are defined as follows. The length is taken as the dimension of the free edge; the width, as the dimension perpendicular to the free edge; and the skew angle, as the angle formed between the vertical axis (dotted line) and the free edge (see Figure 1). Also, the vehicles are considered to circulate in the direction parallel to the free edge.

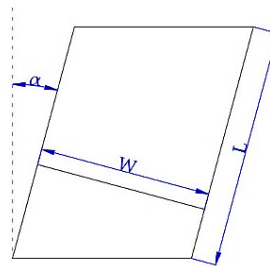


Figure 1. Geometric definition of length, width, and skew angle.

Additionally, the cross section includes the design lane(s), one shoulder and one concrete barrier at each edge, and a 50 mm thick future wearing surface covering the design lane(s) and shoulders. The cross section is kept the same for all 80 case study bridges, with the only distinction the number of lanes. Figure 2 portrays the dimensions for the one lane case study bridge, and the two, three, and four lane cases are analogous.

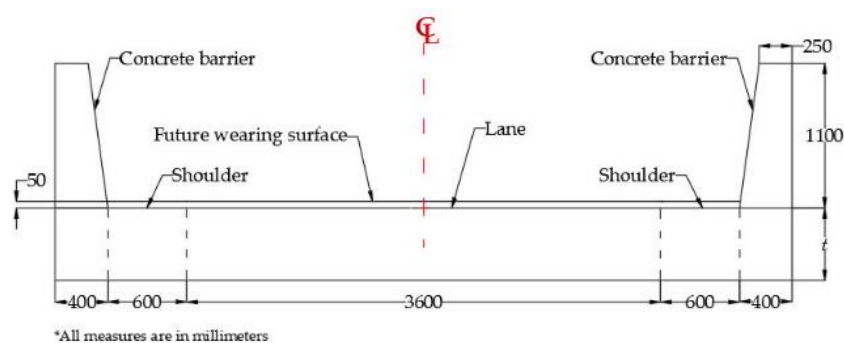


Figure 2. Cross section scheme for the one lane case study bridge.

Concerning materials, 500 MPa yield strength steel and 35 MPa compressive strength concrete are used to analyze and design a total of 80 case study bridges. The length is varied from 7.5 m to 15 m in increments of 2.5 m. Then, the width is varied from 5.6 m (one lane) to 16.4 m (four lanes) in increments of 3.6 m (one design lane). Finally, the skew angle is varied from 0° to 60° in increments of 15°. These 80 configurations are analyzed both through the AASHTO LRFD simplified procedures, using hand calculations, and using LFEA, and are designed using the AASHTO LRFD provisions for the limit state of Strength I. Additionally, for the 16 straight bridges analyzed through the AASHTO LRFD simplified procedures, design is performed as well for the six possible combinations of 500 and 220 MPa yield strength steel and 25, 35, and 60 MPa compressive strength concrete. Likewise, the six material combinations are used for the design of the 7.5 m span, 4 lanes, 15° skew case study bridge and the 15 m span, 2 lanes, and 45° skew case study bridge analyzed with LFEA. All the parameters are summarized in Table 1.

Table 1. Matrix of parameters studied

Length [m]	Number of Lanes	Width [m]	α	f_y [MPa]	f'_c [MPa]
7.5	1	5.6	0°	500	25
10	2	9.2	15°	220	35
12.5	3	12.8	30°	-	60
15	4	16.4	45°	-	-
-	-	-	60°	-	-

1.2. Analysis and Design Procedures

1.2.1. AASHTO LRFD hand calculation

The simplified method from AASHTO LRFD, allows reinforced concrete solid slab bridges, with reinforcement parallel to the direction of the traffic, to be analyzed as a number of interior and exterior simply supported beam type elements (AASHTO, 2017). The loads considered are the following:

DC, is constituted by the self-weight of the slab bridge and by the concrete barriers, and for both a unitary weight of 24.52 kN/m³ is considered. The self-weight of the slab is uniformly distributed along the whole surface, and the weight of the concrete barriers is assumed to act on the exterior strips as done by Rodríguez (Rodríguez, 2017);

- DW, is constituted by the self-weight of the future wearing surface, and a unitary weight of 22.78 kN/m³ is considered. The self-weight is uniformly distributed on top of the design lanes and shoulders;
- LL, is constituted by the vehicular live loading given by the AASHTO HL-93 combination. The lane load is applied as uniformly distributed over a 3.05 m (10 ft) width, and the vehicle loading is applied as point loads generating the most critical moment and shear effects, depending on the phenomenon being analyzed. Also, a dynamic load allowance is applied to the vehicle loading (AASHTO, 2017).

It is worth noting that since the simply supported strips are analyzed as one dimension elements, the self-weight from the DC and DW loading is applied as a uniformly distributed line load over the beam type elements. Furthermore, the procedures for calculating the equivalent strip widths for slab-type bridges are outlined below.

- The equivalent width for interior strips considering one loaded lane is taken as (AASHTO, 2017):

$$E = 10.0 + 5.0\sqrt{L_1 W_1} \quad E(in); L_1(ft); W_1(ft) \quad (1)$$

where E is the equivalent width; L₁, the span of the bridge taken as the lesser of the real span and 18.29 m (60 ft); and W₁, the width of the bridge taken as the lesser of the real width and 9.14 m (30 ft).

- The equivalent width for interior strips considering multiple loaded lanes is taken as (AASHTO, 2017):

$$E = 84.0 + 1.44\sqrt{L_1 W_1} \leq \frac{12.0W}{N_L} \quad E(in); L_1(ft); W_1(ft); W(ft) \quad (2)$$

where E is the equivalent width; L₁, the span of the bridge taken as the lesser of the real span and 18.29 m (60 ft); W₁, is the width of the bridge in feet taken as the lesser of the real width and 18.29 m (60 ft); W, the total width of the bridge taken from edge-to-edge; and N_L, the number of design lanes.

- The reduction factor applied to interior strips of skewed bridges is taken as (AASHTO, 2017):

$$r = 1.05 - 0.25\tan(\alpha) \leq 1.00 \quad (3)$$

where α is the skew angle in degrees. The reduction factor is then multiplied by the equivalent strip widths calculated with (1) and (2), and the greater result is taken as the interior equivalent strip width. Afterwards, the magnitude of the maximum design moment for live load, obtained by loading one design lane with the full HL-93 loading, is divided by the equivalent strip width to get the design live moment for the interior strip (AASHTO, 2017).

- The equivalent width for exterior strips shall be taken as the distance between the inside face of the barrier and the edge of the deck, plus 305 mm (12.0 in), plus a quarter of the strip width. However, it should not exceed 1829 mm (72.0 in) or half the full strip width. Then, the magnitude of the maximum design moment for live load, obtained by considering one line of wheels from the vehicle in the HL-93 loading and a tributary portion of the design lane load, is divided by the equivalent strip width to get the design live load moment and shear for the exterior strip (AASHTO, 2017).

To produce the maximum design moments for flexure design, the moments are taken at midspan for the DC, DW, tandem, and lane load. For the truck, however, the maximum moment is slightly displaced from the midspan and results from positioning the vehicle so that the midspan point of the bridge bisects the distance between the nearest 142 kN (32 k) axle and the center of gravity of the vehicle (Fu, 2013). To produce the maximum design moments and shears for shear design, the moments and shears are taken at the critical shear section. This location is measured perpendicularly at a distance d_v from the support line (see Figure 5.a for reference), where d_v is the effective shear depth calculated as a distance perpendicular to the neutral axis, comprehended between the resultant of the compressive and the resultant of tensile forces due to flexure (AASHTO, 2017). As well, the heaviest axle of the vehicle is positioned at the location of the critical shear section.

With the design magnitudes that come from the analysis, the main longitudinal reinforcement design is provided according to the Strength I limit state. As well, the secondary transverse reinforcement is calculated with the distribution steel provisions from AASHTO LRFD (AASHTO, 2017). Finally, the need for shear reinforcement is verified with the procedures from AASHTO LRFD, which constitute a simplified version of the Modified Compression Field Theory (AASHTO, 2017) (Vecchio, 1986).

1.2.2. Use of linear finite element models

LFEA is performed using SCIA Engineer software version 20.0 (SCIA Engineer, 2018). The solid slab bridges are modeled with isotropic shell elements with hinged line supports in the sides adjacent to the free edges. Also, the mesh size is set to 100 mm for all cases, and the software is set to work with the Mindlin plate bending theory as suggested by Hulsebosch (Hulsebosch, 2019). Additionally, the loads applied in all bridge cases are the same as those described for the simplified methods with a couple of distinctions. First, the vehicle

loading is not applied as point loads but rather as uniformly distributed loads acting over the standard tire contact area (AASHTO, 2017). Second, the multiple presence factor, m , which varies according to the number of loaded lanes and multiplies the magnitude obtained for the live loading, is included (see Table 2) (AASHTO, 2017). This multiple presence factor accounts for the fact that the probability of having multiple lanes loaded simultaneously throughout the design live of the bridge is limited. Third, the barrier is modeled as a uniformly distributed load located along the base width of the barrier in both edges (see Figure 2).

Table 2. Multiple presence factors (AASHTO, 2017)

Number of Loaded Lanes	Multiple Presence Factors
1	1.2
2	1
3	0.85
>3	0.65

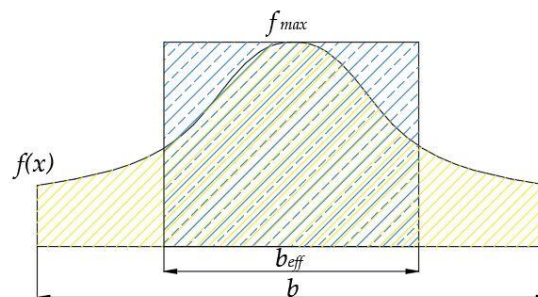


Figure 3. Principle of the effective width applied to moment determination (Lantsoght, 2013).

To produce the maximum design moments for flexure design of the main longitudinal reinforcement, the bending moment for DC and DW is taken as the peak value of the section cut performed perpendicular to the longitudinal direction of the bridge, at the location of maximum longitudinal bending moment, for the corresponding load case (see Figure 5). The bending moment for LL is averaged over the effective width (see Figure 3), defined as a distance where the resisting action caused by the maximum stress distributed along the effective width is the same as the resisting action caused by the variable stresses along the

entire width (Goldbeck, 2017) (Goldbeck, 2016). Also, the live load distribution width is obtained as the weighted average between the live load distribution width and maximum moment in the section cut for the lane and vehicle loading cases.

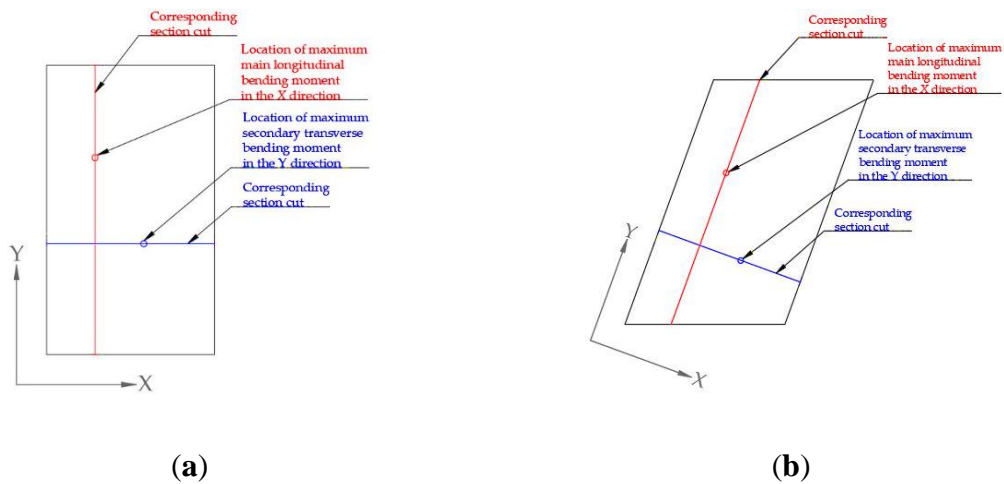


Figure 4. Main longitudinal and secondary transverse moment section cuts for design. (a) Straight bridges; (b) Skewed bridges.

To produce the maximum design moments for flexure design of the secondary transverse reinforcement, a section cut parallel to the longitudinal direction of the bridge, at the location of maximum secondary transverse bending moment, is performed (see Figure 4). Then, the bending moment is obtained through averaging the whole load combination for Strength I limit state over the effective width.

The design moments and shears for shear design are taken at the location of the critical shear section and resolved along the direction of the principal shear stress. To do so, the principal shear force is calculated as follows (Lipari, 2019):

$$v_0 = \sqrt{v_x^2 + v_y^2} \quad (4)$$

Then, the direction of the critical shear force, which is expected to be comparable to the skew angle, is given by (Lipari, 2019):

$$\theta_0 = \arctan\left(\frac{v_y}{v_x}\right) \quad (5)$$

Finally, the moment resolved in the direction of the principal shear force is calculated as (Lipari, 2019):

$$m_0 = m_x \cos^2 \theta_0 + m_y \sin^2 \theta_0 + 2m_{xy} \cos \theta_0 \sin \theta_0 \quad (6)$$

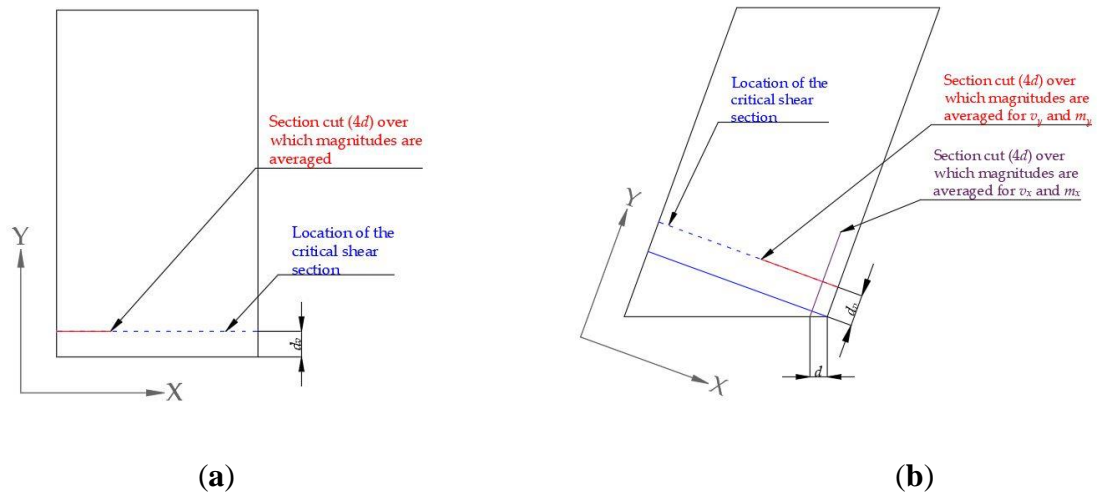


Figure 5. Shear section cuts for design. (a) Straight bridges; (b) Skewed bridges.

Because the magnitudes for shear and moment at the critical shear section proved to be mesh dependent, they are averaged over a width of 4 times the effective depth to the main longitudinal reinforcement of the slab, d (see Figure 5). This width of distribution is selected after Lantsoght, who conducted a study to determine the appropriate width of distribution for peak shear stresses found when using linear finite element models, and also after the guidelines for the assessment of existing bridges in the Netherlands (Lantsoght, 2017) (Rijkswaterstaat, 2013).

Replicating the design considerations from the last section, the reinforcement design is provided according to the Strength I limit state. Then, it is checked whether the distribution steel, which covered the secondary transverse moment effects in the straight bridges, is sufficient to fulfill the secondary transverse moment demands as the skew increases. Finally, the need for minimum shear reinforcement is determined. To do so, it is worth noting that the

area of main longitudinal reinforcement is resolved in the direction of the principal shear strength as follows (Lipari, 2019):

$$A_{s_{calc},\alpha_x}(\theta_0) = A_{s,\alpha_x} \cos^4(\theta_0 - \alpha_x), \quad (7)$$

where θ_0 represents the direction of the principal shear stress, and α_x the direction of the skew angle, but taken from the horizontal x axis. As well, a comparison is made between the nominal shear capacity of the section with the main flexural reinforcement parallel to the direction of the traffic, and the capacity of a section where a virtual rotation of the main flexural reinforcement has been done so that it is perpendicular to the support line. This comparison aims to validate the design procedure of taking moments and shears in the direction of the principal shear stress and utilizing an equivalent main flexural reinforcement steel area (Lipari, 2019).

2. Results and Analysis

This section begins with a brief insight on how steel yield strength from the reinforcement and compressive strength from the concrete influences the design of straight simply supported slab bridges analyzed and designed with AASHTO LRFD. Afterwards, a comparison is made between the maximum longitudinal bending moments from AASHTO LRFD and LFEA, and main longitudinal reinforcement provision, comparing LFEA and interior strips AASHTO LRFD, is discussed as well. Then, the widths of distribution for live load yielded by LFEA are contrasted with the total width of the cross section as defined in Figure 1. Subsequently, an analogous comparison as for longitudinal bending moments is made for secondary transverse bending moments. Next, shear demand and shear capacity is compared for both AASHTO LRFD and LFEA to determine when minimum shear reinforcement is needed. Finally, the design provisions for the two case study bridges designed with different materials are reviewed. At this point it is worth noting for obtaining all design

magnitudes, using LFEA, considered in this study, all of the lanes (1, 2, 3, or 4, respectively) were loaded with the AASHTO HL-93 loading. This decision was taken because when analyzing the bridges with AASHTO LRFD simplified procedures, the multilane loading was shown to be more critical for all 80 case study bridges except, of course, for one lane case study bridges.

It is worth noting that solely the Resistance I limit state is considered for the design of all the bridge cases presented in the entire results and analysis section. This decision is taken because the fulfillment of the Service I limit state would have signified the need for placing the reinforcement in two layers, in some cases, and even requiring a higher slab depth, in others. Thereby, these variations would have impeded one-on-one comparisons as aimed for the study.

2.1. Influence of Steel Yield Strength and Concrete Compressive Strength

One fifth of the 80 case study bridges analyzed and designed with AASHTO LRFD were straight, i.e., with 0° skew angle. These, apart from being designed for 35 MPa concrete and 500 MPa steel, as the rest of the 80 case study bridges, are designed for the six possible combinations of 500, 220 MPa yield strength steel and 25, 35, and 60 MPa compressive strength concrete. Regarding main longitudinal bending moments, it is seen that as long as the bridges maintain the same length, number of lanes, and yield strength steel, the reinforcement provisions for main longitudinal reinforcement, in terms of spacings and bar diameters, are the same. In fact, concrete compressive strength barely influences the theoretical area of required steel, and the difference between 25 MPa and 60 MPa concrete bridges is in the order of 5%, with the demand for 25 MPa being just slightly superior. This is explained by the fact that the influence of concrete compressive strength, used to calculate the internal lever arm from the stress block at the ultimate limit state, is minimal when computing flexural capacity with sectional analysis.

Furthermore, related to secondary transverse reinforcement, the same trend as for main longitudinal reinforcement is witnessed. However, this was already expected because AASHTO LRFD provides an empirical equation that stipulates secondary transverse reinforcement area based exclusively on the length of the bridge (AASHTO, 2017).

Moreover, it is observed that none of the case study bridges in this subsection require minimum shear reinforcement. However, it is worth noting that the 16 bridge configurations that present the lowest shear capacity, when compared to demand, are those with 25 MPa concrete and 500 MPa steel. Such condition was expected since concrete shear capacity from a cross section with no shear reinforcement is mainly driven by the square root of the concrete compressive strength. As well, a section that uses higher yield strength steel requires less area of steel for flexural reinforcement. This leads to higher net longitudinal tensile strains, reducing the parameter β that is directly proportional to concrete shear capacity.

2.2. Maximum main longitudinal bending moment

Figure 6 compares the results of LFEA and AASHTO LRFD in terms of maximum main longitudinal bending moment. The data points for LFEA are specific to each case study bridge; nonetheless, those for AASHTO LRFD represent upper and lower bounds. As it is seen that AASHTO LRFD design moments are higher for exterior than interior strips, the dashed line for exterior strip consists of the upper bound design moments; and the dashed line for interior strip, the lower bound. General trends without span length distinction are the following. First, the exterior strip AASHTO LRFD design moment, for same length and width case study bridges, is the same for all skew angles. Second, the interior strip AASHTO LRFD design moment, for the same length and width case study bridges, decreases slightly as the skew angle increases. Third, the LFEA design moment, for the same length and width case study bridges,

decreases significantly as the skew angle increases, with the exception of a subtle increase with 15° skew angles when compared to 0° skew angles.

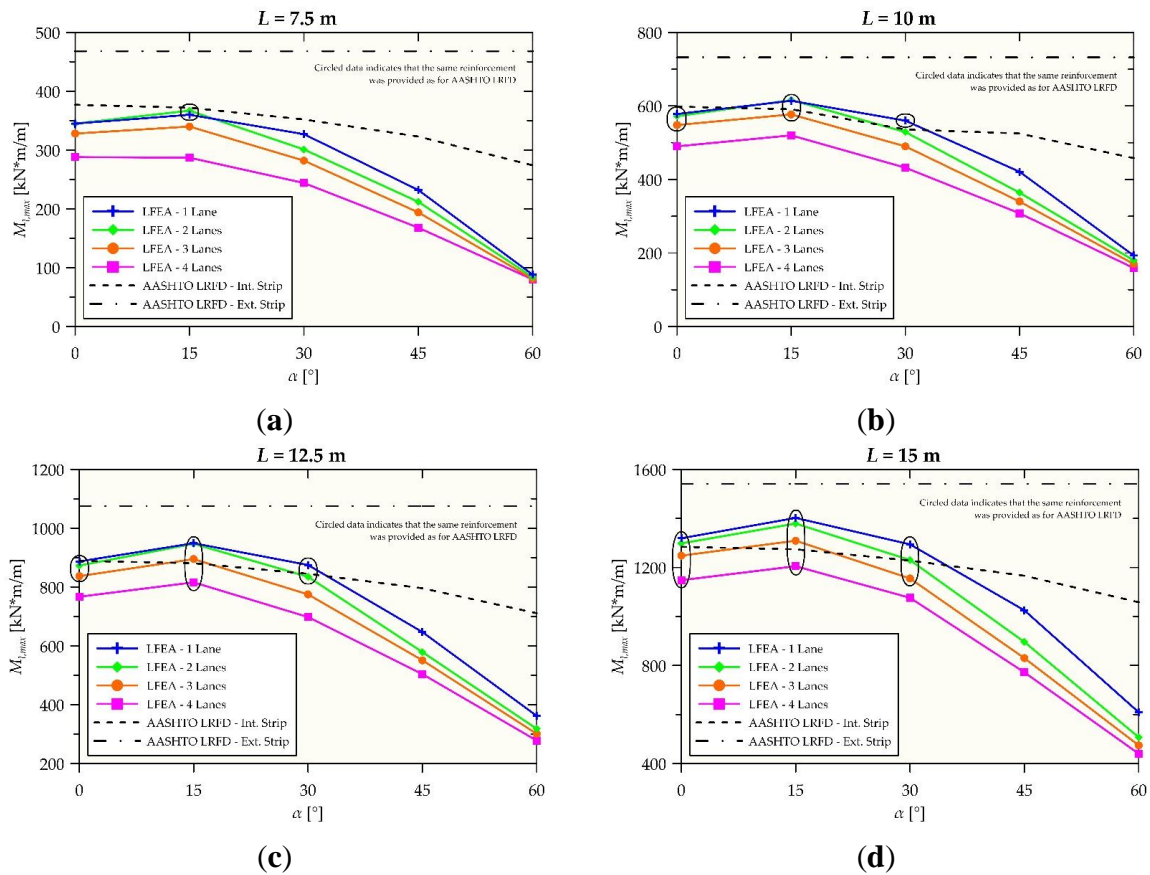


Figure 6. Comparison of LFEA and AASHTO LRFD maximum main longitudinal bending moment. (a) $L = 7.5$ m; (b) $L = 10$ m; (c) $L = 12.5$ m; (d) $L = 15$ m.

Table 3 summarizes the results from Figure 6. The first two columns indicate the percentage by which AASHTO LRFD simplified procedures overestimate the interior and exterior strip $M_{1,max}$ when compared to the LFEA $M_{1,max}$ for the 0° skew angle case study bridges. However, since the percentage varies depending on the number of lanes, an average is presented in the table. Then, the next two columns indicate the percentage by which the $M_{1,max}$ is reduced for the 60° skew angle case study bridges when compared to the 0°. For the simplified procedures, the interior strip $M_{1,max}$ is considered.

In general, for the great majority of case study bridges, independent of length, the overestimation produced by AASHTO LRFD results in smaller spacings or even smaller bar

diameters (see Figure 6). In fact, for the 7.5 m span length the only case study bridges where the same reinforcement is provided is for the one and two lane case study bridges with 15° skew angle. Then, for the 10 m span length the cases where the same reinforcement is provided is for the one, two, and three lane case study bridges with 0° and 15° skew angle, and for the one lane case study bridge with 30° skew angle. Likewise, for the 12.5 m span length the bridges where the same reinforcement is provided is for the one, two, and three lanes straight bridges, all the case study bridges with 15° skew angle, and for the one and two lanes case study bridge with 30° skew angle. For completion, for the 15 m span length the case study bridges where the same reinforcement is provided is for the all the case study bridges with 0° and 15° skew angle, and for the one, two, and three lanes case study bridge with 30° skew angle.

Table 3. Interior and exterior strip $M_{l,max}$ overestimation and $M_{l,max}$ reduction percentage per AASHTO LRFD and LFEA

Length [m]	Interior strip $M_{l,max}$ overestimation	Exterior strip $M_{l,max}$ overestimation	$M_{l,max}$ reduction for 60° skew per AASHTO LRFD	$M_{l,max}$ reduction for 60° skew per LFEA
7.5	22.5%	39.8%	27.9%	75.3%
10	13.9%	33.3%	24.0%	69.8%
12.5	8.9%	28.9%	20.6%	65.1%
15	5.5%	25.1%	18.1%	61.8%

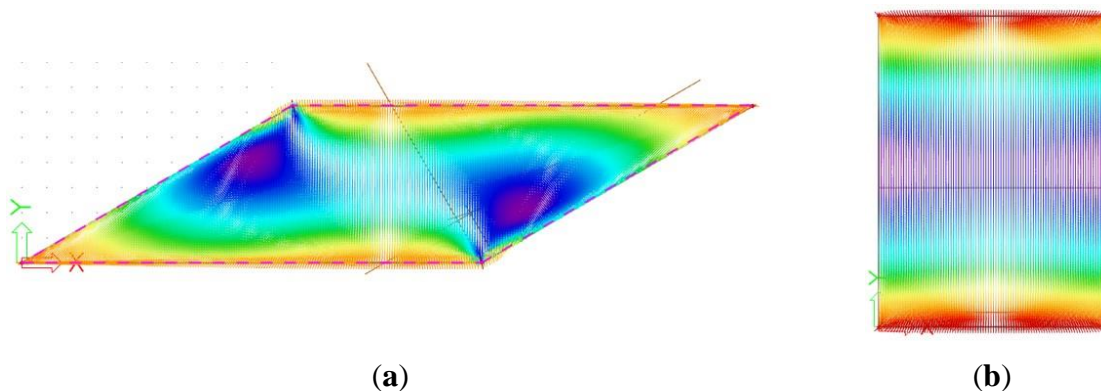


Figure 7. Trajectories of the principal stresses for the 12 m long, 2 lanes case study bridge. (a) Straight $\alpha = 0^\circ$; (b) Skewed $\alpha = 60^\circ$.

The reduction of main longitudinal bending moment that occurs as the skew angle increases is explained by the trajectories of the principal stresses. For straight bridges (see Figure 7.a), the direction of the principal stresses follows the longitudinal direction of the bridge, which causes the main longitudinal bending moments to be higher. However, as the skew begins to grow (see Figure 7.b) the trajectories shift from the main longitudinal to the transverse direction, decreasing the main longitudinal bending moments.

2.3. LFEA live load distribution width for main longitudinal bending moment

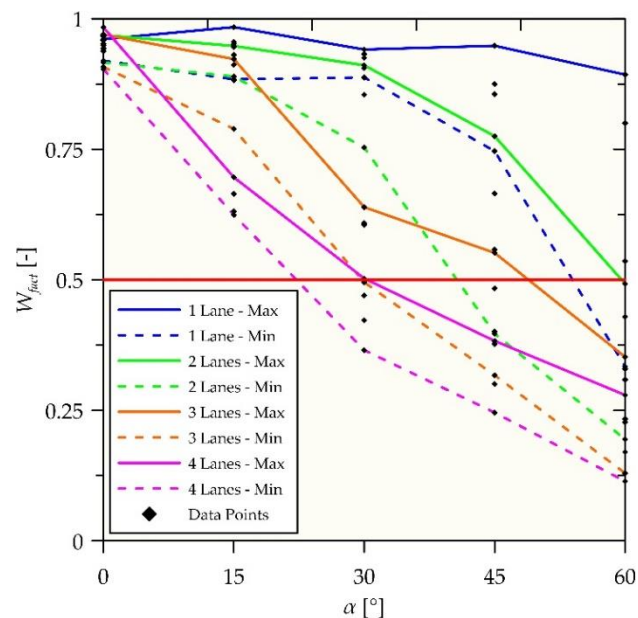


Figure 8. Relation of effective width of distribution for live load, yielded by LFEA, to width of bridge.

Figure 8 contrasts the effective width of distribution for live load yielded by LFEA, as defined in the analysis and design procedures section, W_{eff} , to the width of the bridge, W . By dividing these two magnitudes, the proportion of the width of the bridge that can assume the distribution of live load is determined. For clearness, this proportion will be referred to as width factor, W_{fact} , from now on (see Equation 8). Continuous lines signal the upper bound width factor for case study bridges sharing a same number of lanes but different span lengths; and

dashed lines, the lower bound. As well, the data points indicate specific case study bridges, but no distinction is made as to their specific span length. The horizontal line located at 0.5 signals the point in which at least half of the total width of the bridge can assume the distribution of the live load. As shown in Figure 8, the majority of case study bridges can assume a width of distribution greater than half of the full width. In fact, 68 of the 80 case study bridges can assume more than one third of the width; 55, more than one half; and 42, more than three quarters. Additionally, Figure 8 shows that wider bridges, i.e., bridges that have more lanes or bridges with higher skew angles, tend to reach lower percentages than narrow bridges, i.e., bridges that have less lanes or bridges with smaller skew angles. Moreover, it was seen that shorter span bridges can achieve lower width factors than longer span bridges. For instance, while 15 out of the 16 case study bridges with span length of 12.5 m and 15 m can achieve more than 50%, only 11 out of the case study bridges with span length of 7.5 m can do so.

$$W_{fact} = \frac{W_{eff}}{W} \quad (8)$$

As mentioned before, when the skew angle increases the trajectory of the principal stresses shifts away from the longitudinal to the transverse direction; nonetheless, this is not the only effect that the trajectories undergo. In fact, skewness also causes the trajectories of the principal stresses to densify towards the edges of the bridge. This phenomenon responds to the reduction in width factor evidenced as the skew angle increases, because the denser an area is, when compared to its surroundings, the smaller the effective width of distribution.

2.4. Maximum secondary transverse bending moment

Figure 9 compares the results of LFEA and AASHTO LRFD in terms of maximum secondary transverse bending moment. The data points for LFEA are specific to each case study bridge; nonetheless, those for AASHTO LRFD represent upper and lower bounds. While data from LFEA represents the maximum secondary transverse design moment, data from

AASHTO LRFD represents the secondary transverse capacity attained by the distribution reinforcement provisions from the code (AASHTO, 2017). General trends without span length distinction are the following. First, bending moment demands increase considerably from 0° to 30°, they do not vary significantly from 30° to 45°, and they decrease from 45° to 60°. Second, because the bending moment capacity from the upper and lower bounds does not follow the same trend as the demand, it is evident that, as already expected, the capacity from distribution reinforcement provisions is not influenced by the skew. Third, the distribution provisions from AASHTO LRFD are appropriate for all straight case study bridges analyzed with LFEA since the secondary transverse moment demand is well below the upper and lower bounds for the capacity. Fourth, it appears that, in general, the demand for secondary bending moment tends to increase as the number of lanes increases from one to three lanes, and subsequently it decreases from three to four lanes.

Table 4. Increase in LFEA $M_{t,max}$ demand versus AASHTO LRFD capacity

Length [m]	15° skew angle	30° skew angle	45° skew angle	60° skew angle
7.5	23.4%	103.0%	135.8%	45.1%
10	23.7%	87.7%	125.8%	52.1%
12.5	44.1%	108.4%	110.1%	46.7%
15	27.5%	104.9%	162.6%	86.9%

Table 4 summarizes the results from Figure 9. Each column indicates the percentage by which the $M_{t,max}$, calculated with LFEA, exceeds the bending moment capacity achieved when only distribution reinforcement is provided in the secondary transverse direction as required per AASHTO LRFD. However, since the percentage varies depending on the number of lanes, an average is presented in the table.

For the 7.5 m case study bridges it is seen that the AASHTO LRFD distribution reinforcement provisions are only able to match the demand for the one lane and 15° skew angle case study bridge apart, of course, from the straight cases. Then, for the 10 m span length

cases it is seen that the AASHTO LRFD distribution reinforcement provisions are only able to match the demand for the one lane and 15° skew angle case study bridge. Likewise, for the 12.5 m span length bridges it is seen that the AASHTO LRFD distribution reinforcement provisions are not able to match the demand for any of the case study bridges. For completion, for the 15 m case study bridges it is seen that the AASHTO LRFD distribution reinforcement provisions are only able to match the demand for the one lane and 15° skew angle case study bridge.

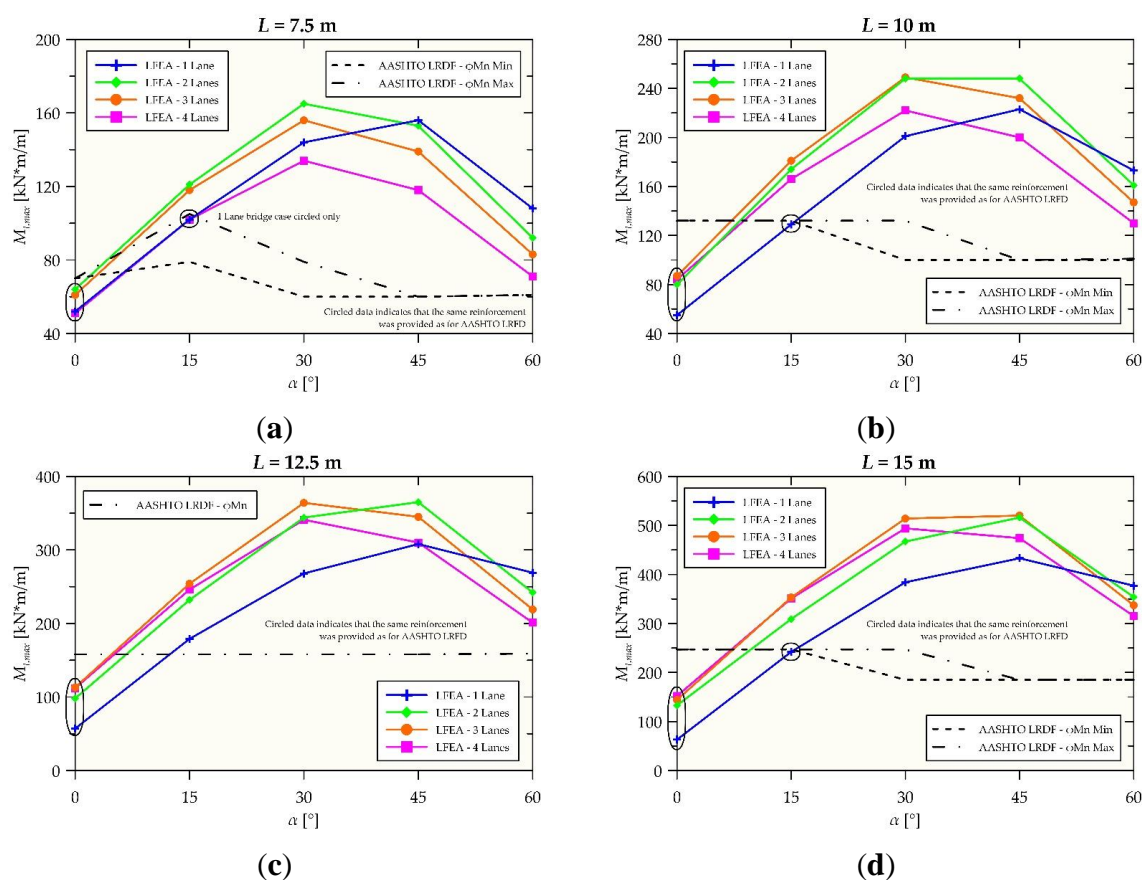


Figure 9. Comparison of LFEA maximum secondary transverse bending moment and AASHTO LRFD bending moment capacity achieved by distribution reinforcement provision. (a) $L = 7.5$ m; (b) $L = 10$ m; (c) $L = 12.5$ m; (d) $L = 15$ m.

The increment of secondary transverse bending moment that occurs as the skew angle increases is explained by the trajectories of the principal stresses. For straight bridges (see Figure 7.a), the direction of the principal stresses follows the longitudinal direction of the bridge, which causes the secondary transverse bending moments to be minimum and taken care

of by the provision of minimum secondary transverse reinforcement. However, as the skew grows and the trajectories shift from the main longitudinal to the transverse direction (see Figure 7.b), the secondary bending moments increase and require more than minimum secondary transverse reinforcement to be withstood.

2.5. Shear demand versus shear capacity

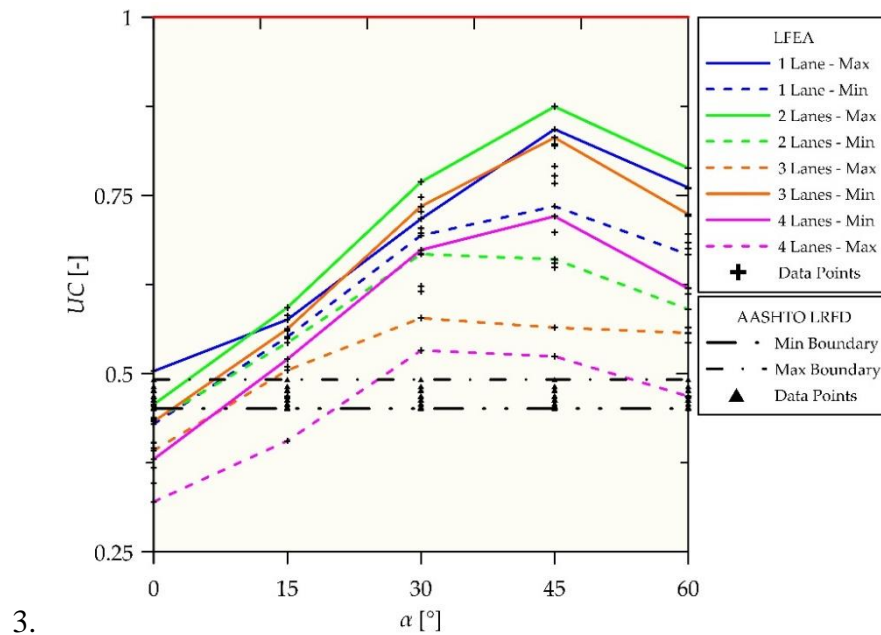


Figure 10. Relation of shear demand to concrete shear capacity with no shear reinforcement.

Figure 10 contrasts the shear demand, V_u , to concrete shear capacity, ϕV_c . By dividing these two magnitudes, the need for shear reinforcement is determined when the division is greater than one. For clearness, this fraction will be referred to as unity check, UC, from now on (see Equation 9). Continuous lines signal the upper bound values for case study bridges sharing a same span length but different number of lanes for LFEA; and dashed lines, the lower bound. On the other hand, dashed horizontal lines show the maximum and minimum boundaries for AASHTO LRFD unity check with no distinction of number of lanes nor span length. As well, the data points indicate specific case study bridges, but no distinction is made as to their specific span length. The horizontal line located at 1 signals the point in which at

least minimum shear reinforcement is necessary to fulfill with the AASHTO LRFD design provisions for shear (AASHTO, 2017).

$$UC = \frac{V_u}{\phi V_c} \quad (9)$$

As shown in Figure 10, none of the case study bridges analyzed with AASHTO LRFD, neither those analyzed with LFEA, showed minimum shear reinforcement requirement, i.e., the highest unity check was seen to be 0.874 for the two lanes, 15 m span and 45° skew angle case study bridge analyzed with LFEA. However, the observable trend for the unity check yielded by AASHTO LRFD varies significantly from that of LFEA. While the trend for AASHTO LRFD is, as expected, not affected by the skew, that from LFEA is to increase considerably from 0° to 30°, either increase or decrease slightly from 30° to 45°, and decrease from 45° to 60°. This behavior is explained by the fact that skewness causes stress concentrations in the obtuse corners. These stress concentrations are translated into substantial shear peak forces that are unobservable in straight geometries. As can be seen, straight case study bridges have significantly lower unity checks than skewed case study bridges, where a slight reduction in concrete compressive strength could potentially lead to minimum shear reinforcement provision needed.

2.6. Particular case study bridges

Two particular case study bridges, analyzed with LFEA, were chosen to be designed for the six possible combinations of 500, 220 MPa yield strength steel and 25, 35, and 60 MPa compressive strength concrete. The selection was arbitrarily made for the 35 MPa compressive strength concrete and 500 MPa yield strength steel bridges with the lowest and highest unity checks to determine how the materials influence reinforcement provision. The bridge with the lowest unity check was the 7.5 m long, 4 lanes, and 15° skew angle; and the bridge with the highest, the 15 m long, 2 lanes, and 45° skew angle. For main longitudinal and secondary

transverse bending moments it is observed that as long as the yield strength for the steel is the same, identical spacings and bar diameters can be specified to fulfill the demands (see Table 5 and Table 6).

Table 5. Reinforcement provision for the 7.5 m long, 4 lanes, 15° skew case study bridge with different material properties

Bridge Case	Material		Main Longitudinal Design		Secondary Transverse Design		Shear Design	
	f'_c	f_y	$A_{s,calc}$ [mm ² /m]	Design	$A_{s,calc}$ [mm ² /m]	Design	UC	Reinforcement
125	2		1621	φ 25mm @ 250mm	591	φ 16mm @ 300mm	0.49	Not needed
109	3	500	1598	φ 25mm @ 250mm	588	φ 16mm @ 300mm	0.41	Not needed
141	6		1576	φ 25mm @ 250mm	585	φ 16mm @ 300mm	0.30	Not needed
173	2		3684	φ 25mm @ 100mm	1350	φ 20mm @ 200mm	0.37	Not needed
157	3	220	3632	φ 25mm @ 100mm	1343	φ 20mm @ 200mm	0.31	Not needed
189	6		3581	φ 25mm @ 100mm	1336	φ 20mm @ 200mm	0.23	Not needed

Table 6. Reinforcement provision for the 15 m long, 2 lanes, 45° skew case study bridge with different material properties

Bridge Case	Material		Main Longitudinal Design		Secondary Transverse Design		Shear Design	
	f'_c	f_y	$A_{s,calc}$ [mm ² /m]	Design	$A_{s,calc}$ [mm ² /m]	Design	UC	Reinforcement
312	25		2947	φ 28mm @ 200mm	1721	φ 20mm @ 150mm	1.05	Needed
296	35	500	2903	φ 28mm @ 200mm	1706	φ 20mm @ 150mm	0.87	Not needed
328	60		2860	φ 28mm @ 200mm	1691	φ 20mm @ 150mm	0.66	Not needed
360	25		6719	φ 32mm @ 100mm	3952	φ 25mm @ 100mm	0.70	Not needed
344	35	220	6618	φ 32mm @ 100mm	3916	φ 25mm @ 100mm	0.58	Not needed
376	60		6519	φ 32mm @ 100mm	3881	φ 25mm @ 100mm	0.44	Not needed

On the other hand, it is seen that the unity check varies significantly as the concrete compressive and steel yield strength change. In fact, this variation can even lead to the need of

providing minimum shear reinforcement as can be seen for bridge case 312 in Table 5. Moreover, as presented in Table 5 and Table 6, lower compressive strengths for the concrete as well as higher yield strengths for the steel lead to higher unity checks.

2.7. Weight of steel reinforcement comparison

This section provides a comparison between the steel needed for the flexural reinforcement of the 80 case study bridges designed with AASHTO LRFD simplified procedures, with hand calculations, and those with LFEA. It is worth noting that for computing the weight it is assumed that the same bar diameters and spacings are provided along the whole width and length of the bridge for the main longitudinal and secondary transverse reinforcement, respectively. For main longitudinal reinforcement, this means that even if for AASHTO LRFD simplified procedures different designs were proposed for interior and exterior strips, those detailed for interior strips were the only ones taken into account herein.

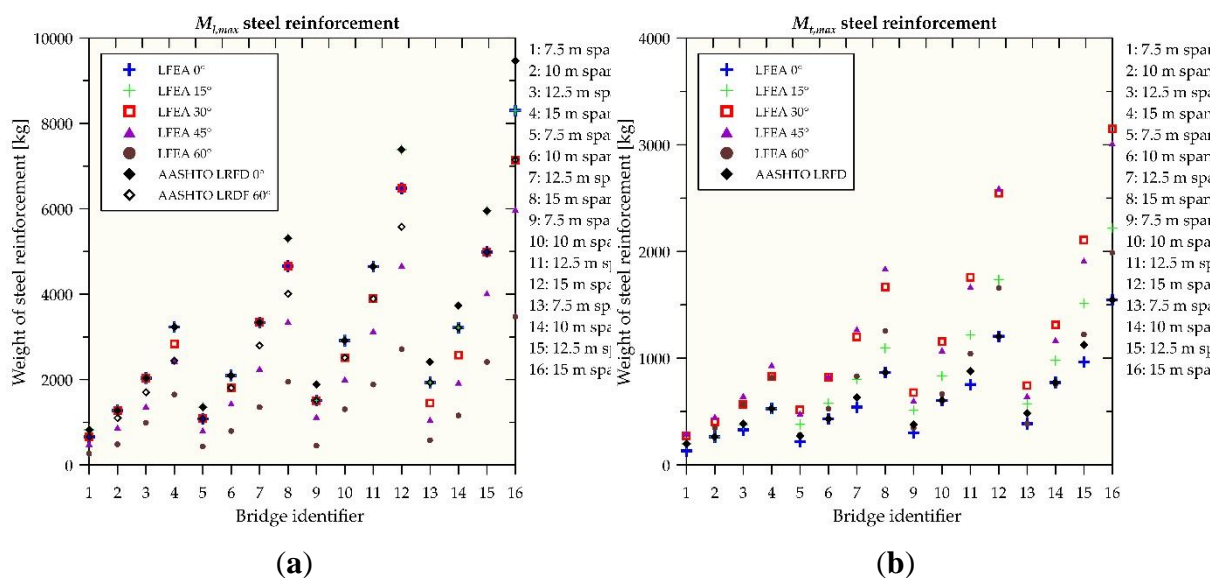


Figure 11. Weight steel reinforcement for bending moment comparison. (a) Main longitudinal; (b) Secondary transverse.

Figure 11.a presents the comparison for main longitudinal reinforcement. As it can be seen, for skew angles up to 15° the difference in weight between the two analysis methods is in the order of 350 kg and 150 kg for 0° and 15° , respectively. However, with increasing skew

angles the difference reaches the order of 600 kg, 1100 kg, and 1500 kg for 30°, 45° and 60°, respectively. In general, AASHTO LRFD resulted in greater steel reinforcement need, with only a few cases equal to LFEA. These cases mainly corresponded to bridges with straight geometries or with a skew angle of 15° (see Figure 6). Then, Figure 11.b presents the comparison for secondary transverse reinforcement. As it can be seen for straight bridges LFEA results in a lower weight of steel, in the order of 50 kg. Nonetheless, as the skew increases, AASHTO LRFD fails to fulfill the reinforcement weight necessary to carry the secondary transverse bending moments. In fact, the difference is in the order of 200 kg, 550 kg, 550 kg, and 150 kg for 15°, 30°, 45°, and 60°, respectively. Finally, Figure 12 establishes an overall summation of main longitudinal and secondary transverse reinforcement to determine the difference between the two analysis approaches in total steel weight. Positive differences indicate a lower total steel weight required by AASHTO LRFD than LFEA and vice versa. It was seen that for most of the 15° and 30° case study bridges, the total steel weight needed per AASHTO LRFD simplified procedures was slightly lower than per LFEA. On the contrary, for the majority of the remaining skewed case study bridges, i.e., those with skew angles of 45° and 60°, the total steel weight needed per AASHTO LRFD simplified procedures was much higher than per LFEA. This is explained by the fact that as the skew angle increases AASHTO LRFD overestimates main longitudinal bending moments and underestimates the required steel to cover secondary transverse moments. In consequence, weight wise speaking, while for the 15° and 30° skew angles the differences between the two analysis methods nearly balance out, for the 45° and 60° skew angles the overestimation of main longitudinal bending moments per AASHTO LRFD simplified procedures by far exceeds the underestimation of secondary transverse steel.

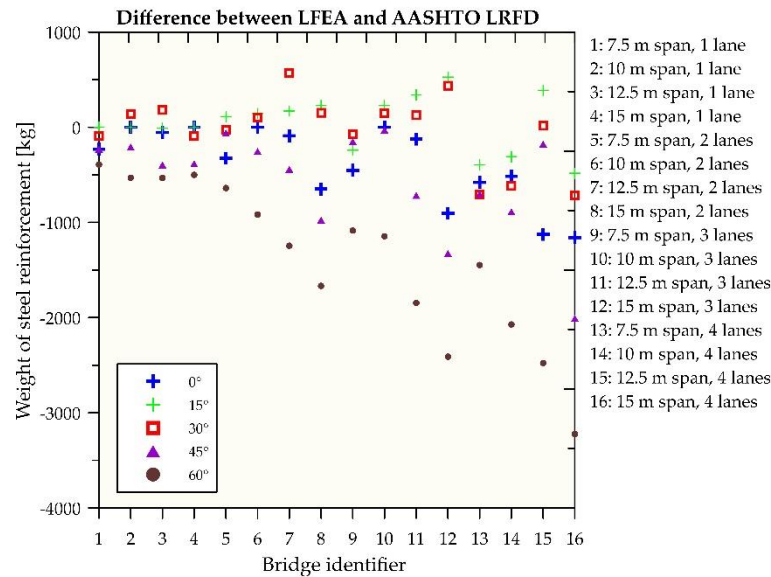


Figure 12. Difference between LFEA and AASHTO LRFD of the summation, in weight, of $M_{l,max}$ and $M_{t,max}$ steel reinforcement.

3. Discussion

The reductions in maximum main longitudinal bending moments, when comparing straight to skewed geometries, aligned with the parametric study conducted by Menassa. While Menassa found that a 50% bending moment reduction was observed for the most skewed case study bridges (Menassa, 2007), i.e., 50°, for the bridges analyzed herein a 45% and 65% bending moment reduction was obtained for the 45° and 60° cases, respectively. However, a notable difference was evidenced in the magnitude of the bending moments from the exterior strips calculated with AASHTO LRFD. Exterior strip bending moments were smaller than those of interior strips (Menassa, 2007). Nonetheless, in the present study, all exterior strip bending moments were higher. This difference could be explained by the fact that while Menassa did not consider concrete barrier loading, the present study did consider concrete barrier loading and assumed it acted solely on the exterior strips, when using AASHTO LRFD simplified procedures with hand calculations, as done by Rodríguez (Rodríguez, 2017). However, after determining the width factor with LFEA it was concluded that assuming the barrier acts solely on the exterior strips can be overly conservative for exterior strip design,

since the slab bridges evidenced a great distribution capacity. In consequence, it is suggested to distribute the weight of the barrier over the entire slab width when using code simplified procedures.

On the other hand, the moment reduction coefficients developed by Théoret were not directly comparable to the moment reductions observed in this study, because those were computed for the relation of width over length (Théoret, 2012). For such motive, even though both studies indicate a pronounced main longitudinal bending moment reduction as the skew angle increases, the results of this study would have to be further processed to enable a direct comparison.

A common trend was observed for the secondary transverse bending moments, computed with more refined analysis than AASHTO LRFD simplified procedures, from the parametric studies from Théoret and Menassa. While these moments were practically negligible for straight geometries, they increased significantly as the skewness grew (Théoret, 2012) (Menassa, 2007). However, the trend in this study varied. While it held true that secondary transverse bending moments were only negligible for straight geometries, these moments magnitude rose from 0° up to 30° or 45° , depending on the case study bridge, and then a significant decrease was observed at 60° . This difference in trend could be explained by how the width of the bridge is accounted for in the studies. Both Théoret and Menassa considered the width of the bridge to be invariant to the skew; nonetheless, the present study considered the width to be measured perpendicular to the free edge and thus dependent on the skew as it related to the physical lane layout and driving direction. In consequence, even if when the skew increases the trajectories of the principal stresses shift towards the secondary direction, they do not concentrate as much because the wider width allows for more distribution.

It is openly recognized that notwithstanding the extensive research that has been done regarding shear behavior of concrete members, there is no clear agreement on a particular design approach (Lipari, 2019). For such reason, this study followed the design provisions from AASHTO LRFD based on the Modified Compression Field Theory (Vecchio, 1986), and applied the design recommendations from Lipari and Lantsoght to the mentioned provisions (Lipari, 2019) (Lantsoght, 2017). The proposals from Lipari were taken one step further to comprehend how the suggestions from his research impact shear reinforcement provision in simply supported reinforced concrete slabs. The obtained design moments and shears showed that none of the 80 case study bridges analyzed necessitated minimum shear reinforcement. However, the LFEA procedure was able to capture the stress concentrations, close to the critical shear section at the obtuse corner, as the skew increased. In consequence, due to the high unity checks obtained for most of the case study bridges, it was agreed that minimum shear reinforcement should be provided close to the edges of the obtuse corner as a conservative measure that will also enhance shear ductility of the bridge (Théoret, 2012). As well, because the design procedure from Lipari was validated (Lipari, 2019) for all case study bridges, it can be recommended for use in practice when designing simply supported reinforced concrete skewed slab bridges.

In general it was seen that the effects analyzed were influenced by the increase in width that took place due to the manner in which width was defined, as previously explained. Future studies could evaluate the same parameters that this parametric study considered, but define the width of the bridge parallel to the support line, since the results from this study suggest that transverse moments as well as shear forces would further increase with this modifications. As well, the position of the truck for shear analysis was taken, as suggested in AASHTO LRFD, at a location of 600 mm away from the barrier. However, since the closer a load is to the edge the more the loads get magnified at the obtuse corner, it would be interesting to verify the shear

demand with a more critical truck positioning. Also, in future studies it is recommended to conduct experiments on skewed slabs to get a better understanding of the behavior of these slabs at the ultimate limit state.

Finally, because this parametric study aimed at providing a practical comparison between AASHTO LRFD simplified procedures and LFEA, a final section was added to analyze how the different design provisions for both main longitudinal and secondary transverse reinforcement would influence the total steel weight wise. This comparison was thought important because the literature reviewed did not account for it. As it was seen in Figure 12, in gross terms LFEA enable steel reduction while guaranteeing the fulfillment of secondary transverse bending moment demand. Also, it is worth noting that shear reinforcement weight was not accounted for since its provision would be minimal considering that the present study suggests its provision solely at the free edges, along the distance where the AASHTO LRFD design provisions suggest extending shear reinforcement past the critical shear section.

CONCLUSIONS

In spite of their span length limitation, slab bridges are widely used around the world. Even though straight geometries are preferable, occasionally urban or geographical constraints make the selection of skewed geometries necessary. In consequence, this paper presented the results of a parametric study intended to determine the applicability of AASHTO LRFD for simply supported reinforced concrete skewed slab bridges. For such purpose, a total of 80 case study bridges, whose varying parameters were length, width, and skew angle, were subjected to the AASHTO HL-93 loading. The bridges were analyzed with the AASHTO LRFD simplified procedures, using hand calculations, and with LFEA from the software package SCIA Engineering. Afterwards, reinforcement provision in terms of main longitudinal, secondary transverse, and shear reinforcement was determined according to the AASHTO LRFD for the analysis methods mentioned herein.

To begin with, regarding main longitudinal bending moments, comparisons between the two analysis methods showed that the simplified code provisions were unable to accurately capture the reduction in moment magnitudes, occasioned by the deviation of the principal stresses from the longitudinal direction, due to the increase in skew angle. It was seen that AASHTO LRFD and LFEA main longitudinal bending moments were only comparable for skew angles up to 15° . Avoiding the consideration of reduced moment yielded augmented steel reinforcement, which would inevitably increase the associated costs. Nonetheless, safety would not be a concern as the provision of additional steel, for these scenarios, would be conservative.

Along the same lines, LFEA exposed that slab bridges have a great distribution capacity of the main longitudinal bending moment. This was evidenced by the width factors which, for most case study bridges analyzed, suggested that the same main longitudinal bending moment reinforcement could be provided for the entire width of the bridge. Moreover, the case study

bridges where the width factors were smaller corresponded to highly skewed bridges. In a great majority of these cases, the main longitudinal bending moment's reduction was so significant, when compared to straight geometries, that minimum flexural reinforcement drove the design. In consequence, providing one only reinforcement would still be valid and conservative. Translating this observations to the field is useful since maintaining one single design provision for main longitudinal reinforcement would represent faster reinforcement layout capability and a reduction in possible reinforcement layout misplacement.

Then, regarding secondary transverse bending moments, comparisons between the two analysis methods indicated that the minimum transverse steel required by the AASHTO LRFD simplified procedures is not sufficient to fulfill secondary transverse bending moment demands for other than straight bridges. Because minimum transverse reinforcement does not take skewness into account, the shifting of the principal stresses towards the transverse direction is not reflected in the design. Evading the provision of this extra secondary transverse reinforcement would result in unsafe designs, since the slab bridges would lack the flexural capacity to resist the mentioned bending moments.

Afterwards, regarding shear forces, comparisons between the two analysis methods verified that the shear capacity of concrete alone was enough to withstand the shear demand for the 80 case study bridges analyzed. However, the unity check obtained with LFEA, unlike such computed through AASHTO LRFD, was far greater for skewed than for straight bridges because of the stress concentration focalized close to the obtuse corner. Thereby, the utilization of slightly lower concrete compressive strengths could inevitably lead to the need for minimum shear reinforcement. In consequence, it is recommended to provide minimum shear reinforcement at the critical shear section of skewed bridges, found next to the obtuse corner, and extend it along the free edge for the required distance according to AASHTO LRFD design provisions as a conservative measure.

Finally, weight wise comparisons showed that for most of the case study bridges analyzed the flexural reinforcement provisions from LFEA, considering both reductions in main longitudinal reinforcement and augmented secondary transverse reinforcement, lead to a lower total weight of steel. As well, it was seen that for the bridge cases where this does not hold true, the overestimation of main longitudinal and underestimation of secondary transverse reinforcement by AASHTO LRFD nearly balance out with the LFEA design. This suggests that LFEA can both represent an economy wise attractive alternative, for the reduction in steel weight, and safety wise attractive alternative, for the enhanced secondary transverse moment capacity and potential minimum shear reinforcement provision requirement.

REFERENCES

- AASHTO. (2017). AASHTO LRFD Bridge Design Specifications, 8th ed.; AASHTO: Washington, DC, USA.
- Fu, G. (2013). *Bridge Design & Evaluation LRFD and LFR*; John Wiley & Sons, Inc.: New Jersey, USA.
- Goldbeck, A.T. (1917). The influence of total width on the effective width of reinforced concrete slabs subjected to central concentrated loading. *ACI Journal Proceedings*, 13(2), 78-88.
- Goldbeck, A.T. and Smith, E.B. (1916). Tests of large reinforced concrete slabs. *ACI Journal Proceedings*, 12(2), 324-333.
- Hulsebosch, C.J.F. (2019). A parametric study on the design of reinforced concrete, simply supported skewed slab highway bridges. Master thesis, TU Delft, Netherlands, pp. 29-55 and 95-129
- Lantsoght, E.O.L., De Boer, A., and Van der Veen, C. (2017). Distribution of peak shear stress in finite element models of reinforced concrete slabs. *Engineering Structures*, 2017, 148(2017), 571-583.
- Lantsoght, E.O.L. (2013). Shear in Reinforced Concrete Slabs under Concentrated Loads close to Supports. Doctoral thesis, TU Delft, Netherlands, pp. 9-36.
- Lipari, A. (2020). A comparative study of shear design methods for straight and skew concrete slabs. *Engineering Structures*, 208(2020), 1-16.
- Massicotte, B. (2007). Étude des causes de l'effondrement du pont du boulevard de la Concorde (in French). Presented at Commission d'enquête sur l'effondrement du viaduc de la Concorde, Montréal, Canada.
- Menassa, C., Mabsout, M., Tarhini, K., and Frederick, G. (2007). Influence of Skew Angle on Reinforced Concrete Slab Bridges. *Journal of Bridge Engineering*, 12(2), 205-214.
- Mitchell, D., Marchand, J., Croteau, P., and Cook, W. (2011). Concorde Overpass Collapse: Structural Aspects. *Journal of Bridge Engineering*, 25(6), 545-553.
- Rijkswaterstaat. (2013). Guidelines Assessment Bridges – assessment of structural safety of an existing bridge at reconstruction, usage and disapproval (in Dutch), RTD 1006:2013 1.1. Utrecht, the Netherlands: 117
- Rodríguez, A. (2017). *Puentes con AASHTO-LRFD 2014 (7th Edition)*, Prometeo Desencadenado, Perú.
- SCIA Engineer Basics Terminology, layout, settings, basic working tools. Available online: https://help.scia.net/download/18.0/en/Basics_enu.pdf (accessed on 5 January 2021).

- Sharma, M., Kwatra, N., and Singh, H. (2019). Predictive Modelling of RC Skew Slabs: Collapse Load. *Structural Engineering International*, 29(3), 443-452.
- Théoret, P., Massicotte, B., and Conciatori, D. (2012). Analysis and Design of Straight and Skewed Slab Bridges. *Journal of Bridge Engineering*, 17(2), 289-301.
- U.S. Federal Highway Administration. U.S. Federal Highway Administration's 2020 National Bridge Inventory data, 2020. Available online: <https://www.fhwa.dot.gov/bridge/nbi/ascii2020.cfm> (accessed on 8 April 2021).
- Vecchio, F.J. and Collins, M.P. (1986). The Modified Compression-Field Theory for Reinforced Concrete Elements Subjected to Shear. *ACI Journal*, 83(2), 219-231.

APPENDIX A: NOTATION

$A_{s,calc}$	Area of steel calculated from flexural design
E	Equivalent width for interior and exterior strips
L	Span length taken as the dimension of the free edge
L_1	Modified span length
$M_{l,max}$	Maximum main longitudinal bending moment
$M_{t,max}$	Maximum secondary transverse bending moment
N_L	Number of lanes
UC	Unity check defined as the ratio of ultimate shear demand to concrete shear capacity
V_u	Ultimate shear demand
W	Width taken as the dimension perpendicular to the free edge
W_1	Modified width
W_{eff}	Effective width for main longitudinal bending moment
W_{fact}	Width factor defined as the ratio of effective width for main longitudinal bending moment to width of the bridge
X	Direction of the x-axis
Y	Direction of the y-axis
b	Full width of a section cut
b_{eff}	Effective width of a section cut
d	Effective depth to the main longitudinal reinforcement
d_v	Effective shear depth
$f(x)$	Function describing the unitary bending moment or shear force along a section cut
f_{max}	Peak unitary bending moment or shear force within a section cut
m	Multiple presence factor
m_o	Magnitude of bending moment in the direction of the principal shear force
m_x	Magnitude of bending moment in the x direction
m_{xy}	Magnitude of torsion effects along the x direction
m_y	Magnitude of bending moment in the y direction
r	Reduction factor for main longitudinal bending moments
v_o	Magnitude of principal shear force
v_x	Magnitude of shear force in the x direction
v_y	Magnitude of shear force in the y direction
α	Skew angle in degrees formed between the y-axis and the free edge
α_x	Skew angle in degrees formed between the x-axis and the free edge
ϕ	Bar diameter dimension
θ_o	Angle between the x-axis and the direction of the principal shear force
ϕV_c	Concrete shear capacity